scientific reports

Check for updates

OPEN

Nsp1 stalls DNA polymerase α at DNA hairpins

Andrey G. Baranovskiy, Lucia M. Morstadt, Nigar D. Babayeva & Tahir H. Tahirov✉

The human primosome, a four-subunit complex of DNA primase and DNA polymerase alpha (Polα), plays a critical role in DNA replication by initiating RNA and DNA synthesis on both chromosome strands. A recent study has shown that a major virulence factor in the SARS-CoV-2 infection, Nsp1 (non-structural protein 1), forms a stable complex with Polα but does not affect primosome activity. Here we show that Nsp1 inhibits DNA synthesis across inverted repeats prone to hairpin formation. Analysis of current structural data revealed the overlapping binding sites for Nsp1 and the winged helix-turn-helix domain of RPA (wHTH) on Polα, pointing to a potential competition between them. Comparison of the inhibitory effect of Nsp1 and wHTH on DNA hairpin bypass by Polα showed an eightfold lower IC_{50} value for Nsp1 (1 µM). This study provides valuable insight into the mechanism of inhibition of human DNA replication by Nsp1 during a SARS-CoV-2 infection.

The SARS-CoV-2 coronavirus is the causative agent of the COVID-19 (Coronavirus disease-2019) pandemic, which had a devastating impact on public health and the global economy. SARS-CoV-2 dysregulates the immune inflammatory response and is characterized by organ dysfunction, high levels of cytokines, and lymphopenia[1]. Nsp1 is a major virulence factor for SARS, which plays an important role in the suppression of the innate immune response[2,3]. Nsp1 mainly targets the Type 1 interferon (IFN-1) signaling pathway, which activates hundreds of genes responsible for the antiviral response[4]. Nsp1 inhibits phosphorylation of STAT1, a signal transcription protein, which forms a heterodimer with STAT2 and associates with the regulatory factor IRF9, resulting in formation of the IFN-stimulated gene factor 3[5].

In addition, Nsp1 inhibits the IFN-1 response by blocking the expression of host proteins in different ways. Nsp1 interacts with the nuclear pore complex and inhibits the export of nuclear mRNA into the cytoplasm[6,7]. Nsp1 also facilitates the degradation of host mRNA by recruiting cellular nucleases[8,9]. Also, Nsp1 binds near the mRNA entry channel of the 40S ribosome subunit and inhibits the initiation of translation[10,11]. At the same time, structural features of viral RNAs allow them to escape Nsp1-mediated degradation and inhibition of translation[3].

The SARS-CoV-2 protein interaction map, published in 2020, shows that the human primosome is a potential target for Nsp1[12]. Intriguingly, among all DNA replication factors, only the primosome, the hetero-tetrameric complex of primase and DNA polymerase α (Polα), is targeted by SARS-CoV-2. The cryoEM structure of the complex of human primosome with a small globular domain of Nsp1 revealed that Nsp1 interacts with an exonuclease domain of Polα[13]. Nsp1 docked away from the active site and the DNA-binding cleft of Polα and showed no effect on its DNA polymerase activity.

The primosome initiates synthesis of every DNA strand by making the chimeric RNA–DNA primers required for loading the main DNA replicases[14,15]. During self-regulated intramolecular primosome reactions, primase synthesizes de novo the RNA primer, which is then extended by Polα with deoxyribonucleotides. Polα belongs to the B-family of DNA polymerases and contains catalytic and accessory subunits. The catalytic domain of human Polα ($Polα_{CD}$, residues 335–1244) adopts the universal "right-hand" DNA polymerase fold containing the following domains: N-terminal, exonuclease, "palm", "thumb", and "fingers"[16]. The exonuclease domain does not possess a 3'-exonuclease activity and plays a structural role.

Recently we have shown that RPA, a single-strand DNA-binding protein, is critical for the human primosome and Polα during DNA synthesis across inverted repeats[17]. RPA is composed of three subunits: RPA70, RPA32, and RPA14, and contains four DNA-binding domains, resulting in a high affinity to DNA[18,19]. The C-terminus of RPA32 contains the flexible wHTH domain (residues 178–270, including the linker), which interacts with different DNA-dependent enzymes including Polα[20–22].

We recently reported the cryo-EM structure of the RPAcore/$Polα_{CD}$/DNA complex, which uncovered the flexible mode of RPA-Polα interaction where the wHTH domain plays a critical role[17]. According to biochemical studies, this domain is essential for RPA-Polα cooperation and DNA synthesis across hairpins[17]. Strikingly, superposition of RPAcore/$Polα_{CD}$/DNA and Nsp1/primosome complexes revealed overlapping binding sites on Polα for wHTH and Nsp1 (Fig. 1). This finding points to a potential role of Nsp1 in the disruption of the RPA-

Eppley Institute for Research in Cancer and Allied Diseases, Fred and Pamela Buffett Cancer Center, University of Nebraska Medical Center, Omaha, NE, USA. ✉email: ttahirov@unmc.edu

Polα interaction, resulting in the primosome stalling at DNA hairpins. To evaluate this hypothesis, we compared the wHTH-Polα and Nsp1-Polα interaction interfaces and conducted biochemical studies demonstrating the inhibitory effect of Nsp1 on hairpin bypass by the RPA/Polα$_{CD}$ complex. Inhibitory assays have shown that Nsp1 forms a more stable complex with Polα than the wHTH domain does, which is consistent with the analysis of the corresponding interaction interfaces.

Results and discussion

Comparison of interaction interfaces between Polα and Nsp1, and between Polα and the wHTH-domain of RPA, indicates that the contact area is larger in the Nsp1/Polα complex (Fig. 2). There are five potential H-bonds between Polα and the wHTH-domain, with involvement of Glu610, Thr617, Arg616, His658, and Lys661 of Polα and Ser250, Asn251, Tyr256, Thr258, and Val259 of RPA (Fig. 2A). At the Nsp1-Polα interface, there are eight potential H-bonds, with contribution from Polα residues Lys599, Ala613, Thr614, Arg616, Thr617, Lys628, and Lys655 and Nsp1 residues Arg24, Asp33, Glu41, His45, Aspn48, and Gly49 (Fig. 2B). Of note, Asp33 of Nsp1 may form salt bridges with Arg616 and Lys655 of Polα. The side chains of two Polα residues, Arg616 and Thr617, participate in H-bonding with both Nsp1 and the wHTH-domain. Three wHTH residues, Tyr256, Thr258, and Thr267, are involved in hydrophobic interactions with Polα (amino acids Thr617, Gly620, Phe621, and Ala624) (Fig. 2C). The same Polα residues interact with Nsp1, with the addition of Ala613 (Fig. 2D). The hydrophobic Polα-binding interface of Nsp1 is formed by six residues: Leu27, Val28, His45, Thr50, Pro109, and Val111.

As we showed previously[17], the nine base-pair (bp) hairpin stalls Polα$_{CD}$, which requires RPA for efficient hairpin bypass (Supplementary Fig. S1 and Fig. 3, lanes 1–3). Intriguingly, addition of Nsp1 significantly inhibits DNA synthesis across the hairpin by the RPA/Polα$_{CD}$ complex (Fig. 3, lanes 4–6). Replacement of the conserved residue Val28 with aspartate, a mutation known to disrupt the Nsp1/Polα complex[13], almost completely recovered the hairpin bypass (Fig. 3, lanes 7–9). These results indicate that the inhibitory effect of Nsp1 on DNA synthesis across inverted repeats is mediated by its specific interaction with Polα.

The wHTH domain also inhibits hairpin bypass but with a lower efficiency (Fig. 3, lanes 10–12). We compared the inhibitory effect of Nsp1 and wHTH on hairpin bypass by the RPA/Polα$_{CD}$ complex (Fig. 4). The obtained IC_{50} values (1.03 ± 0.04 μM for Nsp1 and 8.14 ± 0.38 μM for wHTH) are consistent with structural data showing more contacts at the Nsp1-Polα interface (Fig. 2). These data indicate that Nsp1 efficiently competes with RPA for interaction with Polα. The effect of Nsp1 on hairpin bypass by the RPA/Polα complex is therefore similar to deletion of the wHTH domain[17].

Polα localizes both in the nucleus and in the cytoplasm[23,24]. Nsp1 is a cytoplasmic protein[12]. A small fraction of Nsp1 was detected in the nucleus of Vero cells 9 h post-infection[25]. The nuclear localization of Nsp1 was also observed in plasmid-transfected cells[6,12,26]. It is possible that Nsp1 binds to Polα in the cytoplasm, and the complex then migrates to the nucleus. The findings of this study allow us to speculate that Nsp1 has the potential to inhibit synthesis of the telomeric C-strand by the CST/primosome complex because the wHTH2 domain of CST binds Polα at the same site as the wHTH domain of RPA (Supplementary Fig. S2)[13,27].

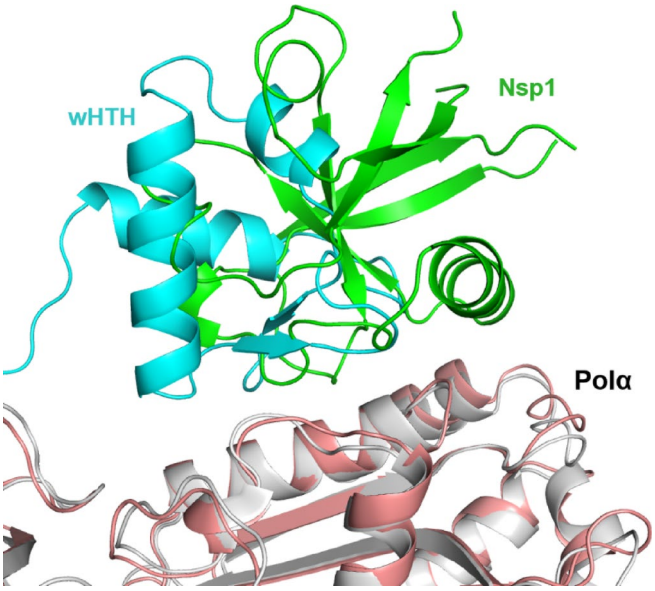

Fig. 1. Nsp1 and the wHTH domain of RPA have overlapping docking sites on Polα. Nsp1, wHTH, and Polα in the complexes with Nsp1 and wHTH are represented as cartoons and colored green, cyan, gray, and salmon, respectively. The coordinates of Nsp1/primosome and RPAcore/Polα$_{CD}$/DNA complexes were used for figure preparation (pdb codes 7opl and 9mj5, respectively). Two complexes were superposed using the Polα region 612–661 involved in interaction. PyMol Molecular Graphics System (version 1.8, Schrödinger, LLC) was used for alignment and figure preparation.

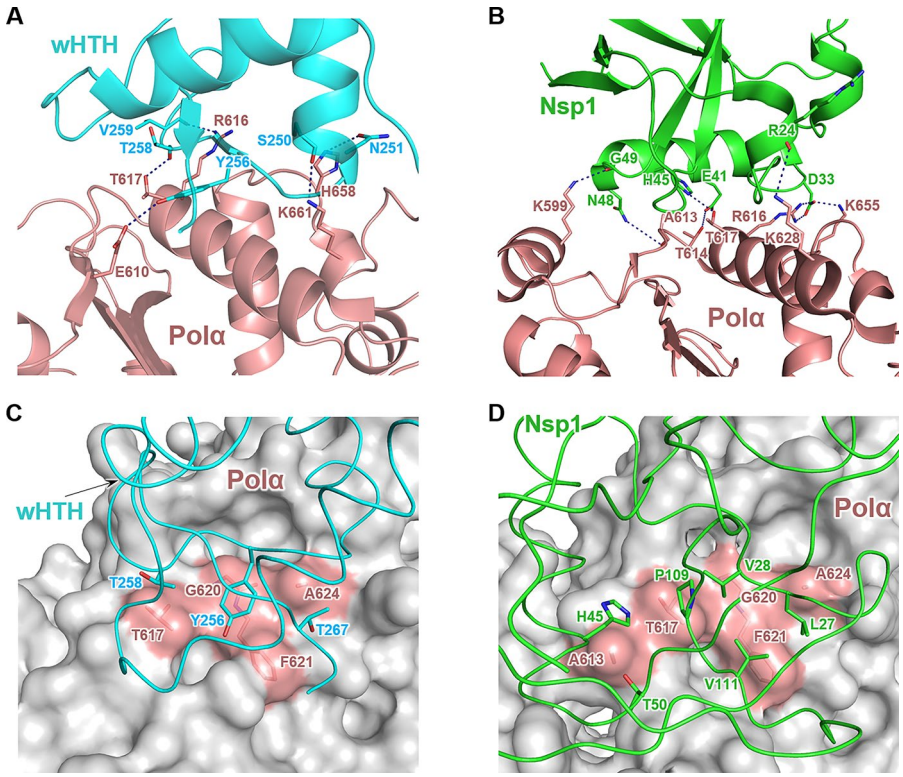

Fig. 2. Nsp1 has a larger interaction interface with Polα than the wHTH domain of RPA. (**A**) and (**B**), analysis of potential hydrogen bonds at the wHTH-Polα and Nsp1-Polα interfaces, respectively. Nsp1, wHTH, and Polα are represented as cartoons and colored green, cyan, and salmon, respectively. H-bonds are depicted as dark-blue dashed lines. A position of the Lys599 side-chain was adjusted for optimal H-bond formation with Gly49 (**C**) and (**D**), analysis of potential hydrophobic contacts at the wHTH-Polα and Nsp1-Polα interfaces, respectively. Polα is represented as a surface. Polα residues, involved in hydrophobic interactions with Nsp1 or wHTH, are shown as sticks and colored salmon. Nsp1 and wHTH are represented as ribbon and colored green and cyan, respectively. Their residues, involved in hydrophobic interactions with Polα, are shown as sticks. PyMol Molecular Graphics System and the coordinates of Nsp1/primosome and RPAcore/Polα$_{CD}$/DNA complexes were used for figure preparation (pdb codes 7opl and 9mj5, respectively).

A deficiency in the catalytic subunits of primase and Polα causes the X chromosome-linked reticulate pigmentary disorder (XLPRD), which is characterized by persistent inflammation, the activation of type I interferon signaling, and recurrent lung infections[28,29]. It was proposed that a reduced level of cytosolic RNA/DNA hybrids triggers this disease, but the molecular mechanism is not well understood[29]. On the other hand, inhibited host DNA replication, mediated by Polα deficiency or inhibition of Polα activity, may cause damage to genomic DNA and the accumulation of replication fork-derived DNA in the cytoplasm, which then stimulates the production of IFN-1 and pro-inflammatory cytokines through the cGAS-STING pathway[30,31]. Interestingly, an abnormal level of cytokines is a hallmark of severe forms of COVID-19, where a dysregulated inflammatory response primarily affects the lungs[1]. The possibility exists that Nsp1 contributes to the development of such symptoms through the inhibition of host DNA replication. In addition, Nsp1 may affect the proliferation of T- and B-lymphocytes and therefore suppress the adaptive immune response against SARS-CoV-2.

Materials and methods

Human RPA and the Polα catalytic domain were obtained as previously described[17]. The expression vector pMCSG53 encoding for the globular domain of Nsp1 SARS-CoV-2 (residues 13–127) with an N-terminal His-tag followed by the Tev-cleavage site was obtained from Addgene (catalog # 167,256) and described in[32]. The Nsp1 variant bearing a point mutation V28D was generated by site-directed mutagenesis. The pASHSUL-1 vector for expression of the wHTH domain was made by inserting the coding sequence for the RPA32 residues 178–270 downstream of the sequence encoding for the His-Sumo tag[33]. Nsp1 and wHTH were expressed in the *Escherichia coli* strain BL21 (DE3) at 16 °C for 15 h following induction with 0.05% α-lactose and 0.3 μg/ml anhydrotetracyclin, respectively. Nsp1 and its V28D variant were purified to near-homogeneity (Supplementary Fig. S3) in two chromatographic steps using Ni-IDA column (Bio-Rad) and Q HiTrap (Cytiva) columns. After the first step, the His-tag was removed by Tev protease during overnight incubation at 4 °C. The wHTH domain of RPA was purified in a similar way, with a His-Sumo tag being digested by dtUD1 protease[33] and removed from the sample by passing through a HisTrap column (Cytiva). The purified proteins were dialyzed against buffer containing 20 mM Tris-Hepes, pH 7.8, 150 mM NaCl, 2% glycerol, and 1 mM TCEP, concentrated to ~ 1 mM,

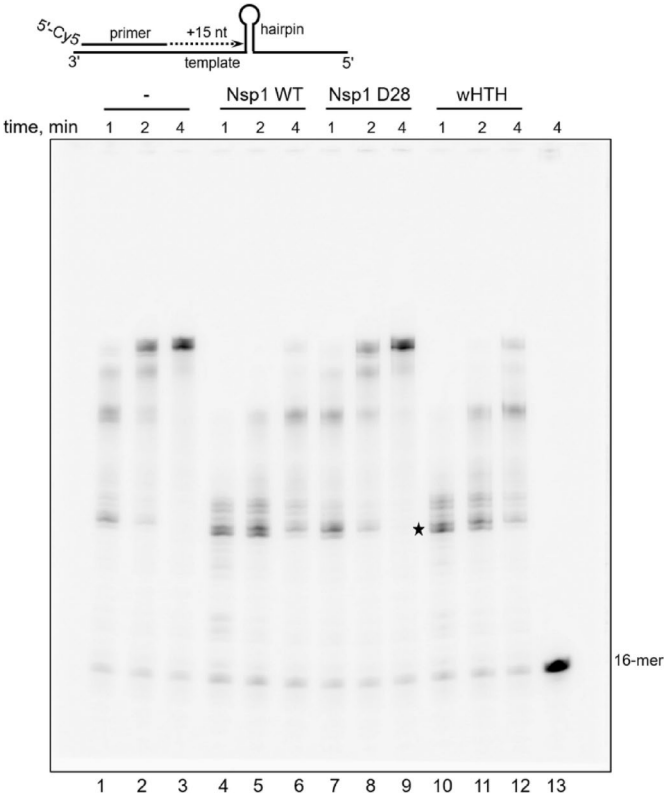

Fig. 3. Nsp1 inhibits DNA synthesis across a 9-bp hairpin by the RPA/Polα complex. The DNA synthesis activity of Polα in extension of a 16-mer DNA primer with a Cy5-fluorophore attached to the 5′-end was tested in a 10 µl reaction containing 0.25 µM template:primer, 20 nM Polα, 0.7 µM RPA, and 25 µM dNTPs; 8 µM Nsp1 or 40 µM wHTH were added as indicated on the figure. Lane 13 is a control incubation in the absence of proteins. The star denotes the pause site at the beginning of a hairpin located 15 nucleotides from the 3'-end of the primer. Reactions were incubated at 35 °C, and the products were resolved by 20% Urea-PAGE and visualized by imaging on Typhoon FLA 9500. The substrate schematic is shown at the top.

and frozen in 10 µl aliquots. Protein concentrations were estimated by measuring the absorbance at 280 nm and using the extinction coefficients calculated with ProtParam[34].

DNA synthesis activity of Polα was tested in 10 µl reactions containing 0.25 µM template:primer, 20 nM Polα, 0.7 µM RPA, 25 µM dNTPs, and the buffer: 30 mM Tris-Hepes, pH 7.8, 120 mM KCl, 30 mM NaCl, 1% glycerol, 1.5 mM TCEP, 5 mM $MgCl_2$, and 0.2 mg/ml BSA. Nsp1 and wHTH were added to the reactions as indicated in the figure legends. The 16-mer DNA primer contains a Cy5 fluorophore attached to its 5′-end. The 73-mer template 5′-AATGATGAAGATATCTGGTCGCTCCATTCT GGAGCGACCTCTTAATCTAAGCACT CGCTATGTTTTCAAGTTT is prone to formation of a 9-bp hairpin (bases contributing to the hairpin stem are shown in *italics*; the primer annealing site is underlined). Reactions were incubated for the indicated time points at 35 °C and stopped by mixing with equal volume of stopper solution containing 90% v/v formamide, 50 mM EDTA, pH 8, and 0.02% Bromophenol blue, heated at 95 °C for 1 min, and resolved by 20% Urea-PAGE. Reaction products were visualized by imaging on Typhoon FLA 9500 (Cytiva) and quantified by ImageJ, version 1.54 (NIH). Experiments were repeated three times.

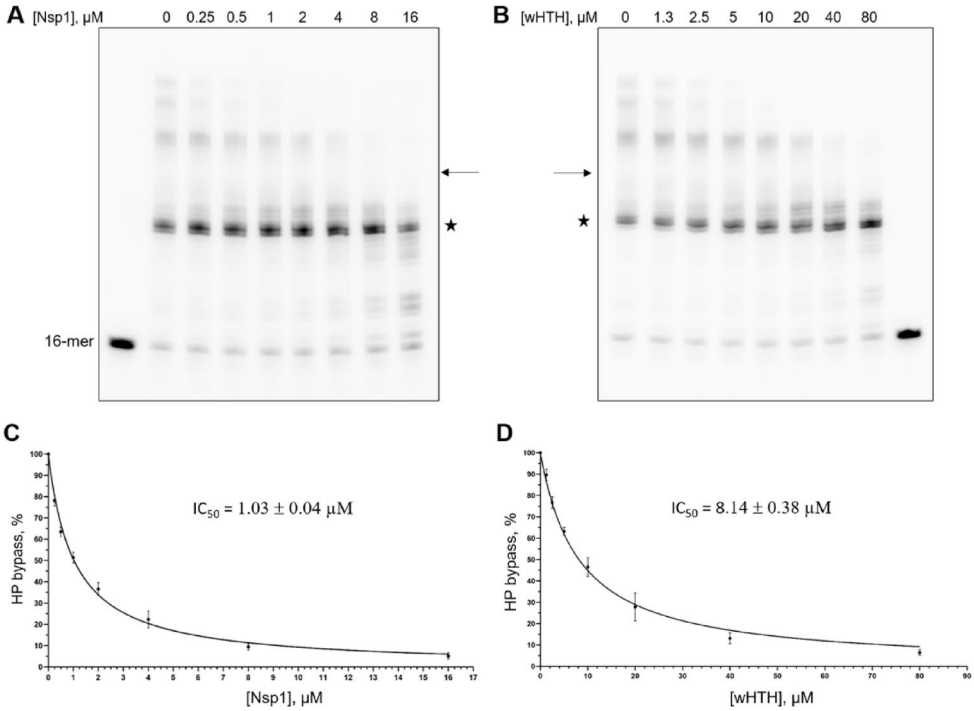

Fig. 4. Comparison of the inhibitory effect of Nsp1 and wHTH on hairpin bypass by RPA/Polα. (**A**) and (**B**), representative gels showing titration of DNA-synthetic activity by Nsp1 and wHTH, respectively. The star denotes the pause site at the beginning of a hairpin. The bands above the arrow were counted as products of hairpin bypass. Reactions were incubated for 1 min at 35 °C, and the products were resolved by 20% Urea-PAGE and visualized by imaging on Typhoon FLA 9500. Original images of the gels are presented in Supplementary Fig. S4. (**C**) and (**D**), the mean value of the percent of hairpin bypass is plotted against Nsp1 and wHTH concentrations, respectively. Error bars denote the standard deviation. The IC_{50} values were calculated from three independent experiments using GraphPad Prism.

Data availability

Data is provided within the manuscript or supplementary information file.

Received: 18 October 2024; Accepted: 2 May 2025
Published online: 21 May 2025

References

1. Li, C., He, Q., Qian, H. & Liu, J. Overview of the pathogenesis of COVID-19 (review). *Exp. Ther. Med.* **22**, 1011 (2021).
2. Narayanan, K., Ramirez, S. I., Lokugamage, K. G. & Makino, S. Coronavirus nonstructural protein 1: Common and distinct functions in the regulation of host and viral gene expression. *Virus Res.* **202**, 89–100 (2015).
3. Yuan, S., Balaji, S., Lomakin, I. B. & Xiong, Y. Coronavirus Nsp 1: Immune response suppression and protein expression inhibition. *Front. Microbiol.* **12**, 752214 (2021).
4. Fisher, T. et al. Parsing the role of NSP1 in SARS-CoV-2 infection. *Cell Rep.* **39**, 110954 (2022).
5. Xia, H. et al. Evasion of type I interferon by SARS-CoV-2. *Cell Rep.* **33**, 108234 (2020).
6. Zhang, K. et al. Nsp1 protein of SARS-CoV-2 disrupts the mRNA export machinery to inhibit host gene expression. *Sci. Adv.* https://doi.org/10.1126/sciadv.abe7386 (2021).
7. Guo, J. et al. Virus infection and mRNA nuclear export. *Int. J. Mol. Sci.* **24**, 12593 (2023).
8. Gaglia, M. M., Covarrubias, S., Wong, W. & Glaunsinger, B. A. A common strategy for host RNA degradation by divergent viruses. *J. Virol.* **86**, 9527–9530 (2012).
9. Karousis, E. D. The art of hijacking: how Nsp1 impacts host gene expression during coronaviral infections. *Biochem. Soc. Trans.* **52**, 481–490 (2024).
10. Lapointe, C. P. et al. Dynamic competition between SARS-CoV-2 NSP1 and mRNA on the human ribosome inhibits translation initiation. *Proc. Natl. Acad. Sci. U. S. A.* https://doi.org/10.1073/pnas.2017715118 (2021).
11. Thoms, M. et al. Structural basis for translational shutdown and immune evasion by the Nsp1 protein of SARS-CoV-2. *Science* **369**, 1249–1255 (2020).
12. Gordon, D. E. et al. Comparative host-coronavirus protein interaction networks reveal pan-viral disease mechanisms. *Science* https://doi.org/10.1126/science.abe9403 (2020).
13. Kilkenny, M. L. et al. Structural basis for the interaction of SARS-CoV-2 virulence factor nsp1 with DNA polymerase alpha-primase. *Protein Sci.* **31**, 333–344 (2022).
14. Baranovskiy, A. G. & Tahirov, T. H. Elaborated Action of the human primosome. *Genes (Basel)* **8**, 62 (2017).
15. Pellegrini, L. The pol alpha-primase complex. *Subcell Biochem.* **62**, 157–169 (2012).
16. Baranovskiy, A. G. et al. Activity and fidelity of human DNA polymerase alpha depend on primer structure. *J. Biol. Chem.* **293**, 6824–6843 (2018).

17. Baranovskiy, A., Morstadt, L., Romero, E. E., Babayeva, N. & Tahirov, T. H. Human primosome requires replication protein A when copying DNA with inverted repeats. *bioRxiv* (2025).
18. Chen, R. & Wold, M. S. Replication protein A: single-stranded DNA's first responder: dynamic DNA-interactions allow replication protein A to direct single-strand DNA intermediates into different pathways for synthesis or repair. *BioEssays* **36**, 1156–1161 (2014).
19. Fanning, E., Klimovich, V. & Nager, A. R. A dynamic model for replication protein A (RPA) function in DNA processing pathways. *Nucleic Acids Res.* **34**, 4126–4137 (2006).
20. Mer, G. et al. Structural basis for the recognition of DNA repair proteins UNG2, XPA, and RAD52 by replication factor RPA. *Cell* **103**, 449–456 (2000).
21. Feldkamp, M. D., Mason, A. C., Eichman, B. F. & Chazin, W. J. Structural analysis of replication protein A recruitment of the DNA damage response protein SMARCAL1. *Biochemistry* **53**, 3052–3061 (2014).
22. Braun, K. A., Lao, Y., He, Z., Ingles, C. J. & Wold, M. S. Role of protein-protein interactions in the function of replication protein A (RPA): RPA modulates the activity of DNA polymerase alpha by multiple mechanisms. *Biochemistry* **36**, 8443–8454 (1997).
23. Nakamura, H., Morita, T., Masaki, S. & Yoshida, S. Intracellular localization and metabolism of DNA polymerase alpha in human cells visualized with monoclonal antibody. *Exp. Cell Res.* **151**, 123–133 (1984).
24. Thul, P. J. et al. A subcellular map of the human proteome. *Science* https://doi.org/10.1126/science.aal3321 (2017).
25. Prentice, E., McAuliffe, J., Lu, X., Subbarao, K. & Denison, M. R. Identification and characterization of severe acute respiratory syndrome coronavirus replicase proteins. *J. Virol.* **78**, 9977–9986 (2004).
26. Shemesh, M. et al. SARS-CoV-2 suppresses IFNbeta production mediated by NSP1, 5, 6, 15, ORF6 and ORF7b but does not suppress the effects of added interferon. *PLoS Pathog.* **17**, e1009800 (2021).
27. He, Q. et al. Structures of the human CST-Polalpha-primase complex bound to telomere templates. *Nature* **608**, 826–832 (2022).
28. Van Esch, H. et al. Defective DNA polymerase alpha-primase leads to X-linked intellectual disability associated with severe growth retardation, microcephaly, and hypogonadism. *Am. J. Hum. Genet.* **104**, 957–967 (2019).
29. Starokadomskyy, P. et al. DNA polymerase-alpha regulates the activation of type I interferons through cytosolic RNA:DNA synthesis. *Nat. Immunol.* **17**, 495–504 (2016).
30. Ragu, S., Matos-Rodrigues, G. & Lopez, B. S. Replication stress, DNA damage, inflammatory cytokines and innate immune response. *Genes (Basel)* **11**, 409 (2020).
31. Yu, L. & Liu, P. Cytosolic DNA sensing by cGAS: Regulation, function, and human diseases. *Sign. Transduct. Target Ther.* **6**, 170 (2021).
32. Semper, C., Watanabe, N. & Savchenko, A. Structural characterization of nonstructural protein 1 from SARS-CoV-2. *iScience* **24**, 101903 (2021).
33. Weeks, S. D., Drinker, M. & Loll, P. J. Ligation independent cloning vectors for expression of SUMO fusions. *Protein Expr. Purif.* **53**, 40–50 (2007).
34. Gasteiger, E., Hoogland, C., Gattiker, A., Duvaud, S., Wilkins, M. R., Appel, R. D. & Bairoch, A. in Walker, J. M. (ed.), *The Proteomics Protocols Handbook* 571–607 (Humana Press, 2005)

Acknowledgements

This work was supported by the National Institute of General Medical Sciences grant R35GM152032 to T.H.T. We thank K. Jordan for editing the manuscript and J. Lovelace for assistance with wHTH/Polα model generation. AlphaFold-multimer modeling was performed at the Holland Computing Center of the University of Nebraska, which receives support from the UNL Office of Research and Economic Development, and the Nebraska Research Initiative.

Author contributions

A.G.B.: Conceptualization, Data curation, Formal analysis, Investigation, Methodology, Validation, Writing—review and editing, Writing—original draft. L.M.M.: Investigation, Methodology, Writing—review and editing. N.D.B.: Investigation, Resources. T.H.T.: Conceptualization, Funding acquisition, Project administration, Supervision, Writing—review and editing. All authors reviewed the manuscript.

Declarations

Competing interests

The authors declare no competing interests.

Additional information

Supplementary Information The online version contains supplementary material available at https://doi.org/10.1038/s41598-025-00982-8.

Correspondence and requests for materials should be addressed to T.H.T.